Downloaded via UNIV OF NEW MEXICO on May 15, 2021 at 12:04:57 (UTC).
See https://pubs.acs.org/sharingguidelines for options on how to legitimately share published articles.

ACS Catalysis

pubs.acs.org/acscatalysis Research Article

Iron-Catalyzed Triazole-Enabled C−H Activation with Bicyclopropylidenes

Jiayu Mo, Antonis M. Messinis, João C. A. Oliveira, Serhiy Demeshko, Franc Meyer, and Lutz Ackermann*

Cite This: *ACS Catal.* 2021, 11, 1053−1064 Read Online

ACCESS | Metrics & More | Article Recommendations | Supporting Information

ABSTRACT: C−H/C−C functionalizations with oxymethylated bicyclopropylidenes were accomplished with an iron catalyst under external oxidant-free conditions. The combination of the unique reactivity of bicyclopropylidenes with a robust iron(II) catalyst enabled C−C cleavages in a chemoselective fashion, which allows for the synthesis of isoquinolones, free isoquinolones, or bispiro-fused isoquinolones. Mechanistic studies provided strong support for the C−C cleavage via *β*-C elimination. A rare monoselective C−F/C−H bond functionalization of trifluoromethylarene was also observed.

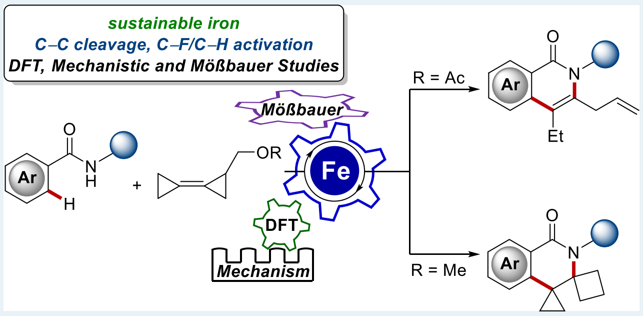

KEYWORDS: *iron, C−H/C−C activation, C−F/C−H activation, BCP, mechanism, Mößbauer study*

INTRODUCTION

Transition metal-catalyzed C−H activation[1−10] has emerged as an increasingly powerful platform for efficient C−C and C−Het formations, with transformative applications to material sciences,[11,12] natural product syntheses,[13,14] and drug discovery.[15−18] While most transformations have thus far been accomplished with precious 4d and 5d metal catalysts, sustainable catalytic manifolds by 3d metal catalysis[19−29] and especially iron-catalyzed C−H transformations[30−46] have attracted significant attention because of their high Earth-abundance, cost-efficiency, and low toxicity.[47] However, despite indisputable progress, iron-catalyzed C−H activations continue to be severely limited.[48−54]

A significant stimulus in C−H activation chemistry was recently gained by combining C−H activation with challenging C−C cleavages.[55−79] Despite considerable achievements, catalytic C−H/C−C functionalizations remain underdeveloped, with the reported examples thus far being largely restricted to precious metal catalysts,[80−89] activated vinylcyclopropanes,[90−93] and harsh oxidative conditions (Scheme 1a, b).[94]

Bicyclopropylidenes (BCPs) have been recognized as increasingly useful structural motifs in modern synthetic chemistry.[95−101] However, despite being accessible via the Kulinkovich cyclopropanation reaction[102] (Scheme 2) and in strong contrast to alkylidenecyclopropanes, their applications in C−H transformations continue to be scarce, with only two ruthenium-catalyzed C−H hydroarylations being reported where the cyclopropane rings were found to be conserved.[103−105] Within our program on sustainable C−C functionalizations,[106,107] we now disclose the first C−H/C−C activation with oxymethylated BCPs catalyzed by Earth-abundant, nontoxic iron. Salient features of our findings include (1) first iron-catalyzed C−H/C−C functionalization, (2) exceedingly mild reaction conditions, and (3) leaving group-enabled chemodivergency (Scheme 1).

RESULTS AND DISCUSSION

We initiated our studies by probing various reaction conditions for the envisioned iron-catalyzed C−H/C−C activation of benzamide **1a** with BCP **2** (Tables 1 and S1 in the Supporting Information). Preliminary studies indicated *i*-PrMgBr, tetrahydrofuran (THF), and 1,2-bis(diphenylphosphino)-ethane (dppe) to be the optimal additive, solvent, and phosphine, respectively (Table S1, entries 5−15 and 33−45), while TAH (triazolylmethyl) was the *N*-substituent of choice because of its unique effectiveness as an orienting group in iron-catalyzed C−H activation.[39,40] The unique reactivity of BCPs was reflected by the judicious choice of the leaving group governing the chemoselectivity. Specifically, when alkyl ethers were employed as leaving groups, bispiro-fused isoquinolone **4ac** was obtained. In sharp contrast, acyloxy-BCP **2f** delivered isoquinolone **3af** (entries 1−6). The C−H/C−C activation occurred efficiently

Received: November 1, 2020
Revised: December 17, 2020
Published: January 7, 2021

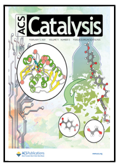

© 2021 American Chemical Society

https://dx.doi.org/10.1021/acscatal.0c04748

Scheme 1. Iron-Catalyzed C–H/C–C Functionalization Sequence with BCPs

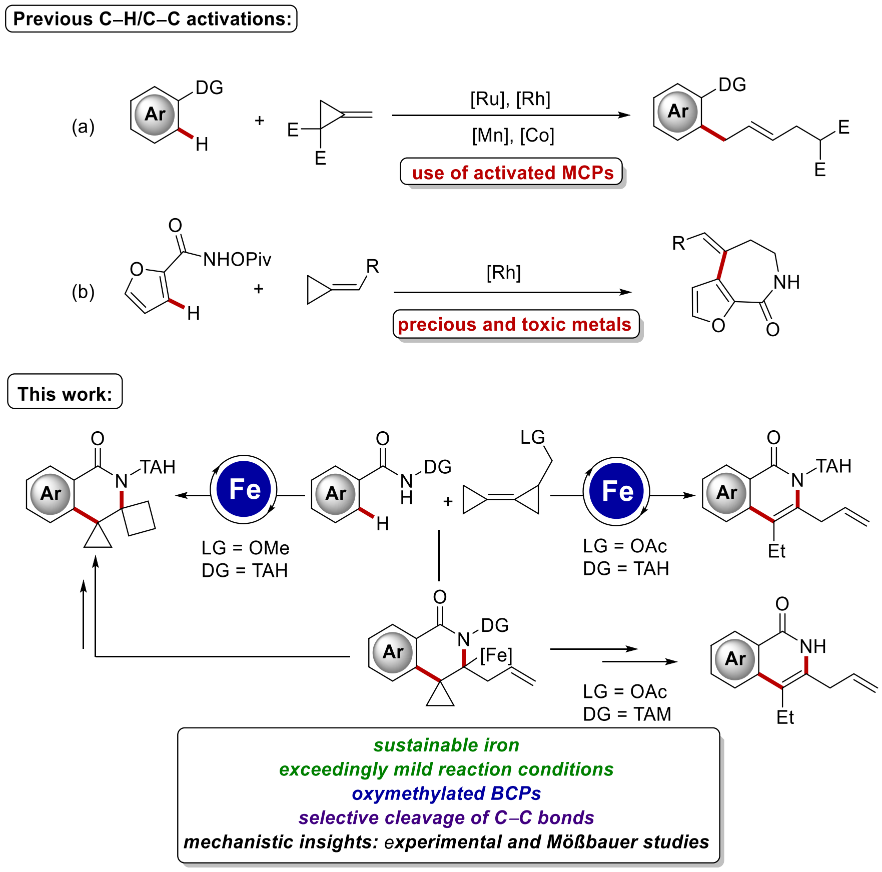

Scheme 2. Synthesis of BCPs

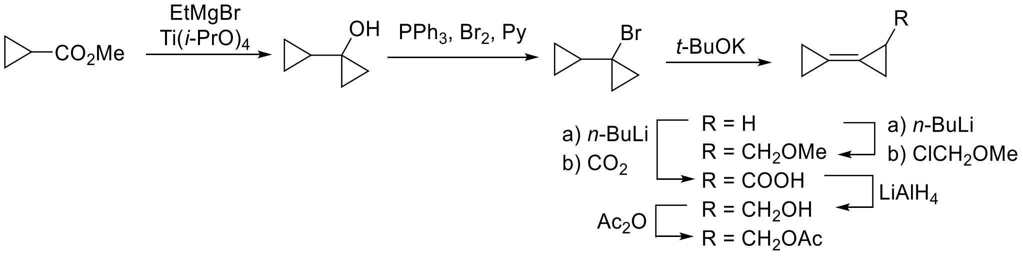

at ambient temperature (entry 7) and without significant decrease in yield when 2 equiv of BCP were used (entry 8).[108] The catalytic reaction worked equally well in 2-MeTHF,[109] while operationally simple $FeCl_2$ could also be employed as a catalyst (entries 9 and 10).

With the optimized reaction conditions in hand (Table 1, entry 6), we subsequently explored the effect of the orienting group on the reaction. According to the results presented in Scheme 3, TAH was found to be superior as an orienting group compared to quinoline or when no orienting group is employed. Therefore, we then explored the versatility of the iron-catalyzed C–H/C–C functionalization with a variety of substituted TAH-benzamides **1** (Scheme 4). Thus, a series of methylene-tethered triazoles delivered the desired isoquinolones **3af–3ef** in moderate to high yields, tolerating among others an otherwise reactive alkyl chloride (**1c**) without any cross-coupling products being observed. Notably, synthetically useful chloro and bromo groups as well as oxidation-sensitive sulfides were fully tolerated (**3hf**, **3jf**, **3mf**, and **3nf**), which should prove valuable for further postsynthetic late-stage diversification. A rare C–F/C–H activation was triggered when the CF_3-*para*-substituted TAH-substrate (**1k**) was employed, providing the C–H/C–C/C–F/C–H functionalized product **3kf′** (see p. S29 for a tentative mechanistic proposal). Additionally, CF_3-*meta*-substituted TAH substrate (**1o**) afforded byproduct **3of′** with conservation of one cyclopropane ring. These findings provide strong support for a β-elimination mechanism to be responsible for the ring opening of the cyclopropanes (vide infra).

The versatile iron catalyst further allowed for the conversion of alkyl- and aryl-substituted BCPs **2g–2h** to furnish the corresponding isoquinolones **3ag–3ah** in moderate yields and excellent regioselectivities.

It is noteworthy that the dimethylmethylene TAM (triazolyldimethylmethyl) group could be directly removed during the catalytic reaction affording free isoquinolones **7** and alkene **8**, eliminating subsequent steps for orienting group removal (see p. S29 for a tentative mechanistic proposal). For

Table 1. Optimization of the Iron-Catalyzed C−H Activation with BCP 2[a]

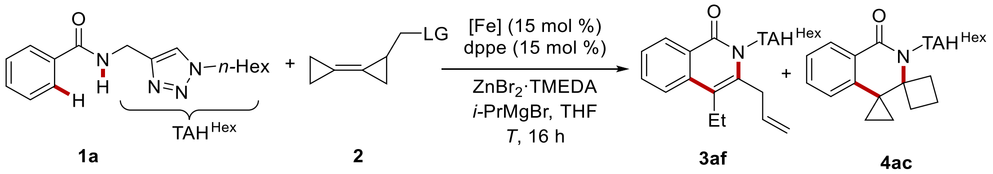

entry	[Fe]	LG	**3af** [%]	**4ac** [%]
1	Fe(acac)$_3$	OBn (**2a**)	-	35
2	Fe(acac)$_3$	OEt (**2b**)	-	<5
3	Fe(acac)$_3$	OMe (**2c**)	-	45
4	Fe(acac)$_3$	OTHP (**2d**)	15	30
5	Fe(acac)$_3$	OC(O)OMe (**2e**)	70	-
6	**Fe(acac)$_3$**	**OAc (2f)**	**80**	-
7	Fe(acac)$_3$	OAc (**2f**)	64[b]	-
8	Fe(acac)$_3$	OAc (**2f**)	70[c]	-
9	Fe(acac)$_3$	OAc (**2f**)	70[d]	-
10	FeCl$_2$	OAc (**2f**)	53[c]	-

[a] Reaction conditions: **1a** (0.30 mmol), **2** (0.90 mmol), [Fe] (15 mol %), dppe (15 mol %), ZnBr$_2$·TMEDA (0.60 mmol), *i*-PrMgBr (0.90 mmol), THF (0.40 mL), 65 °C, 16 h; yields of isolated product. [b] 23 °C. [c] **2f** (0.60 mmol). [d] 2-MeTHF as the solvent. acac = acetylacetonate, dppe = 1,2-bis(diphenylphosphino)-ethane, and TMEDA = *N,N,N′,N′*-tetramethyl ethylene-diamine.

Scheme 3. Effect of the Orienting Group on the Iron-Catalyzed C−H/C−C Functionalization[a]

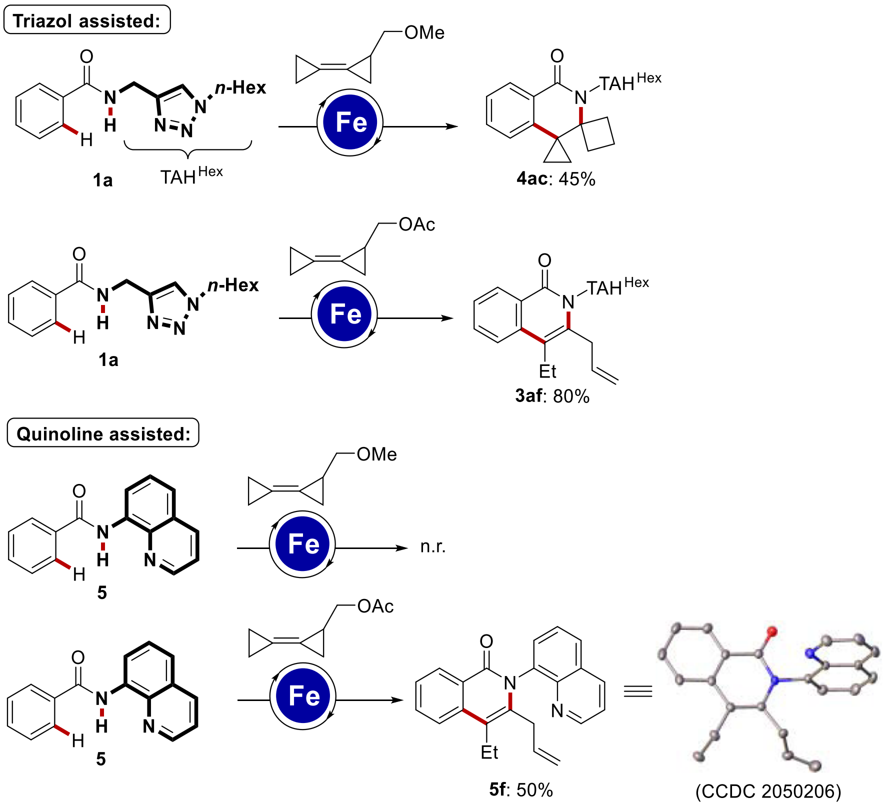

[a] Reaction conditions: entry 3 and entry 6 in Table 1. Monodentate benzamides were found to be unreactive under otherwise identical conditions.

the *para*-CF$_3$ substituted TAM substrate (**6b**), the C−F/C−H functionalization was not observed here, which is suggestive of the C−N bond cleavage taking place preferentially over the C−C cleavage of the second cyclopropane ring during the formation of the free isoquinolone product **7** (Scheme 5).

The unprecedented bispiro-fused isoquinolone **4** could be selectively obtained with OMe serving as the leaving group (Scheme 6). Thus, differently substituted methylene-tethered triazoles delivered the desired spiro-fused product **4** in moderate yields. Notably, the chloro, thioether, and bromo substituents in substrates **1c**, **1h**, and **1n**, respectively, were also well tolerated.

It is also worth noting that the orienting group of product **4ac** was removed in an electro-oxidative fashion (Scheme 7). The molecular structure of the free isoquinolone **9** was unambiguously confirmed by X-ray diffraction analysis, Scheme 4. Iron-Catalyzed C−H/C−C Functionalization with Acyloxy-BCPs 2[a]

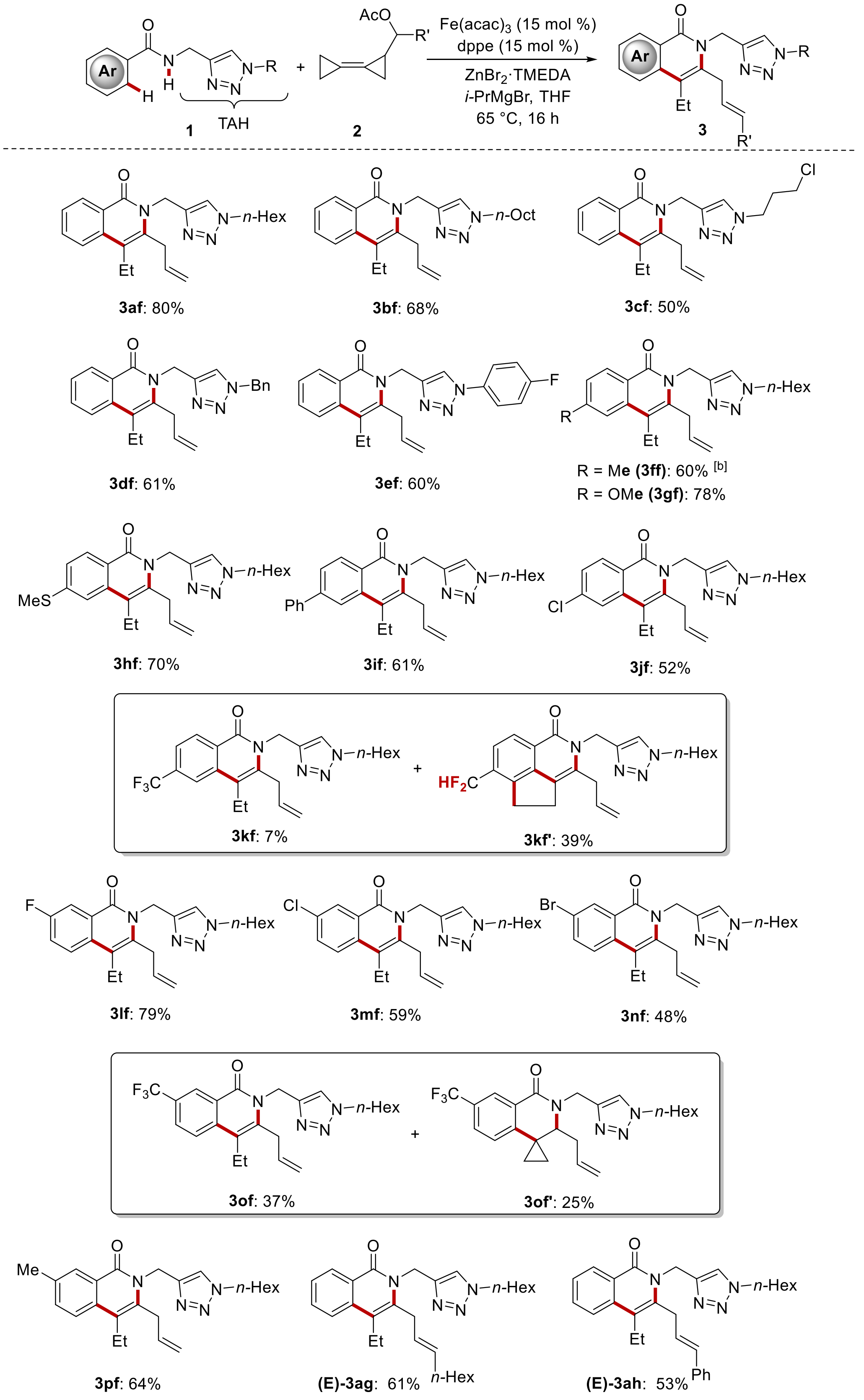

---

[a] Reaction conditions: **1** (0.30 mmol), **2** (0.90 mmol), Fe(acac)$_3$ (15 mol %), dppe (15 mol %), ZnBr$_2$·TMEDA (0.60 mmol), *i*-PrMgBr (0.90 mmol), THF (0.40 mL), 65 °C, 16 h; [b] 55 °C, 36 h.

Scheme 5. Iron-Catalyzed C−H/C−C Functionalization with TAM Removal[a]

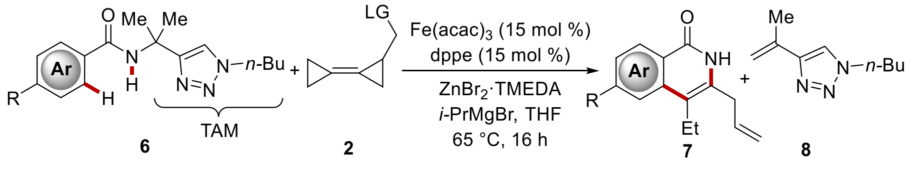

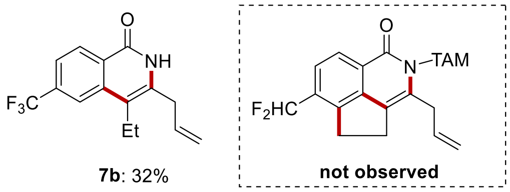

LG	yield **7a** [%]	yield **8** [%]
OMe (**2c**)	---	---
OAc (**2f**)	30	24
OTHP (**2d**)	**52**	**52**

[a]Reaction conditions: **6** (0.30 mmol), **2** (0.90 mmol), Fe(acac)$_3$ (15 mol %), dppe (15 mol %), ZnBr$_2$·TMEDA (0.60 mmol), *i*-PrMgBr (0.90 mmol), THF (0.40 mL), 65 °C, 16 h.

Scheme 6. Iron-Catalyzed C−H/C−C Functionalization with BCP 2c[a]

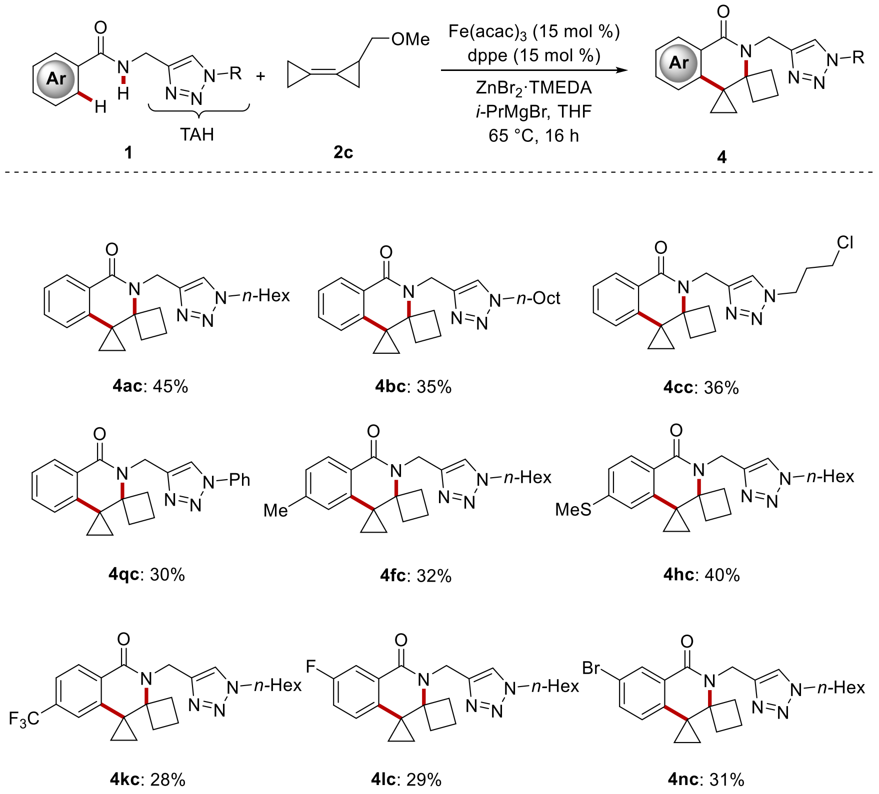

[a]Reaction conditions: **1** (0.30 mmol), **2c** (0.90 mmol), Fe(acac)$_3$ (15 mol %), dppe (15 mol %), ZnBr$_2$·TMEDA (0.60 mmol), *i*-PrMgBr (0.90 mmol), THF (0.40 mL), 65 °C, 16 h.

Scheme 7. Electro-Removal of the TAH Orienting Group

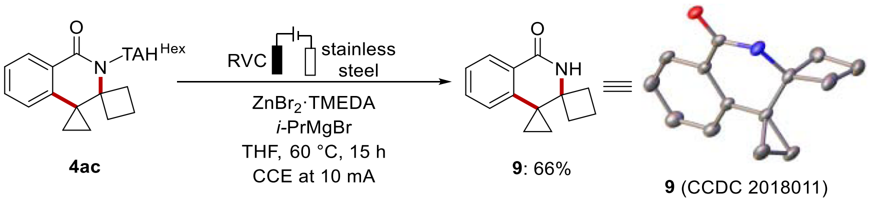

revealing a strained amide bond. The cyclobutane carbon is indeed out of the amide bond plane with a Winkler−Dunitz parameter of τ = 10.8°, which could set the stage for a facile C−N bond scission.[110]

In order to shed light on the reaction mechanism, intermolecular competition experiments were performed. A similar reactivity between electron-deficient and electron-rich arenes **1** (Scheme 8a) was hence observed. The lack of a

Scheme 8. Competition Reaction and KIE Study

(a) Competition Experiment

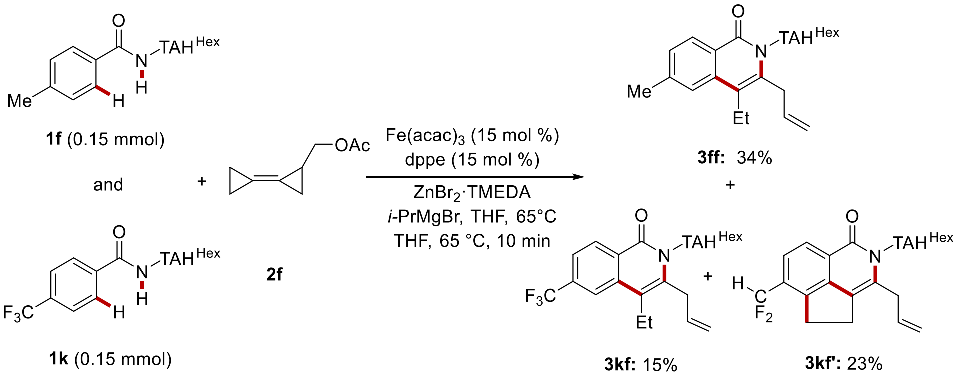

(b) Intermolecular KIE (independent reactions)

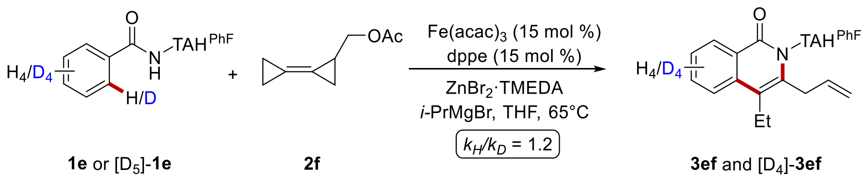

(c) Intermolecular KIE (one-pot)

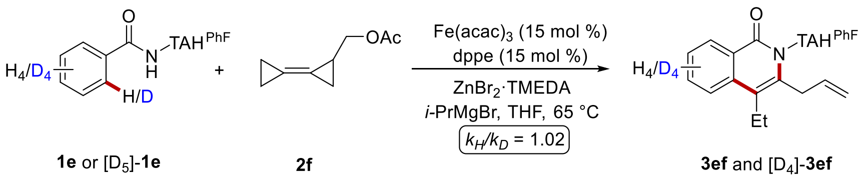

significant kinetic isotope effect (KIE) was noted when the catalytic reaction was performed with isotopically labelled substrate [D$_5$]-**1e**, which supports a facile C−H cleavage (Scheme 8b, c). Moreover, the deuterium-labelled substrate [D$_5$]-**1a** resulted in considerable H/D scrambling in the second ortho-position of the product [D$_n$]-**3af** or [D$_n$]-**4ac**, being indicative of a fast and reversible C−H activation event (Scheme 9a, b). It is proposed that the H in this case originates from the isopropyl group after β-H elimination on the iron center.

Interestingly, deuterium incorporation was position-selective for the corresponding products **3** and **4** (Scheme 9), which indicates an iron-catalyzed C−C functionalization occurring during the catalytic reaction. Partial deuterium incorporation in the products [D]-**3af** and [D]-**4ac** (Scheme 9c, d) indicates that intermediates **E** and **F** could be the resting states for corresponding pathways A and B in the catalytic cycle (Figure 2). In addition, diastero-selective deuterium incorporation in the products [D$_n$]-**4ac** and [D]-**4ac** was observed (Scheme 9b, d), which suggested a migratory insertion taking place for the formation of intermediate **F** (Figure 2, pathway B).

For further understanding of the iron's mode of action, detailed ^{57}Fe Mößbauer spectroscopic studies were conducted to reveal the spin and oxidation states of the dominant iron species. To that end, ^{57}FeCl$_2$ was added to THF solutions containing some or all of the various key components (namely, MeMgBr, ZnBr$_2$·TMEDA, dppe, **1a**, and/or **6a**, **2c**, and **2f**; see Table 2) and after filtration, Mößbauer spectra of the frozen solutions were recorded at 80 K. Isomer shifts δ > 0.9 mm s^{-1} and rather large quadrupole splittings ΔE_Q are indicative of high-spin iron(II) species[111] akin to the ones previously reported by Neidig and co-workers as well as by our group.[39,113] Therefore, it is highly possible that several catalytic intermediates might correspond to high-spin iron(II) species. Nevertheless, the presence of low valent iron transient species cannot be completely ruled out at this stage.[113]

In order to better understand the effect of the leaving group on the observed chemodivergency, density functional theory calculations were carried out at the PW6B95-D4/def2-TZVP//TPSS-D3BJ/def2-SVP level of theory (Figure 1 and p. S40).[114−123] Analysis of the quintet ground state reveals that the intermediate with the methoxyl leaving-group ($\mathbf{D^{OMe}}$) features the olefin tilted away from the methoxyl, which appears favorable for the subsequent alkene migratory insertion. In contrast, the cyclopropyl group of intermediate $\mathbf{D^{OAc}}$ appears to favor a β-C elimination.

Based on our experimental studies and previous findings,[113] we propose the iron(II)-catalyzed C−H/C−C annulation sequence to be initiated by a facile C−H activation via ligand-to-ligand hydrogen transfer[39,124−128] to generate the cyclometalated iron species **A** (Figure 2). After coordination of substrate **2**, intermediate **B** undergoes migratory insertion to deliver complex **C**, which gives intermediate **D** by reductive elimination[126] and β-C elimination. Orienting group and

Scheme 9. Isotopically Labelled Experiments

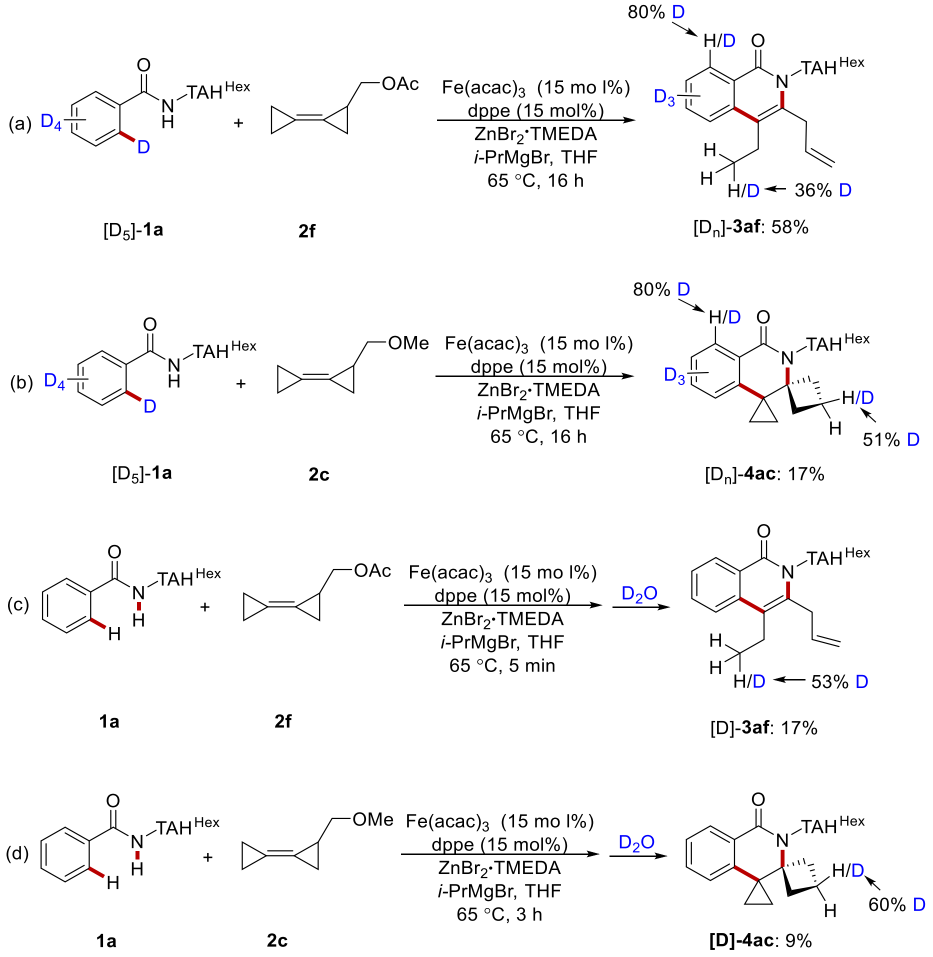

Table 2. ^{57}Fe Mößbauer Parameters of Reaction Mixtures

entry	reaction	valence of iron/spin state	δ (mm s^{-1})	ΔE_Q (mm s^{-1})	rel. int. (%)
1	$^{57}FeCl_2$ + THF	$+2^{HS}$	1.26	3.05	100
2	entry 1 + MeMgBr	+1.4[112]	0.29	0.88	100
3	entry 2 + $ZnBr_2$·TMEDA	$+2^{HS}$	1.01	2.69	69
		$+2^{HS}$	1.36	2.56	31
4	entry 3 + dppe	$+2^{HS}$	0.92	1.42	23
		$+2^{HS}$	0.98	2.57	40
		$+2^{HS}$	1.24	2.68	37
5	entry 4 + **1a**	$+2^{HS}$	0.89	2.05	30
		$+2^{HS}$	0.93	2.63	49
		$+2^{HS}$	1.02	3.07	21
6	entry 5 + **2f**	$+2^{HS}$	0.95	2.22	33
		$+2^{HS}$	1.02	2.79	55
		$+2^{HS}$	1.05	3.13	12
7	entry 4 + **6a** + **2f**	$+2^{HS}$	0.92	2.09	44
		$+2^{HS}$	0.95	2.66	36
		$+2^{HS}$	1.03	3.00	20
8	entry 5 + **2c**	$+2^{HS}$	0.74	2.34	13
		$+2^{HS}$	1.02	2.63	65
		$+2^{HS}$	1.03	3.09	22

leaving group chemodivergency delivers diverse products through different pathways (pathways A and B). For the formation of isoquinolone product **3**, intermediate **D** undergoes β-C elimination (pathway A) and then ligand-to-ligand hydrogen transfer to furnish product **3af**, thereby regenerating the active iron species **A**. With respect to the transformation to bispiro-fused product **4**, instead of a C−C bond cleavage, migratory insertion of the alkene into the iron−carbon bond takes place and forms intermediate **F** (pathway B), which then produces **4ac** and regenerates the active iron species **A**.

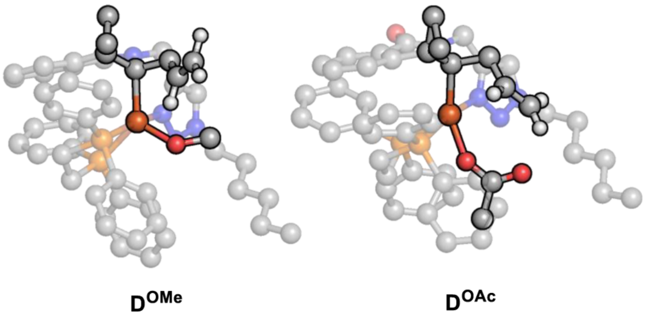

Figure 1. Calculated structures for intermediate **D** at the TPSS-D3BJ/def2-SVP level of theory for the two leaving groups in the high-spin (quintet spin state) ground state. Nonrelevant hydrogens are omitted for clarity.

■ CONCLUSIONS

In summary, we have reported on the first C−H/C−C activation with BCPs by the aid of Earth-abundant, nontoxic iron catalysis. Thus, product formation was governed by the nature of the substitution pattern of the BCPs and provided access to isoquinolones, free isoquinolones, or bispiro-fused isoquinolones. Furthermore, a unique monoselective C−F/C−H activation sequence of trifluoromethylarenes was discovered during our study.

■ ASSOCIATED CONTENT

Supporting Information

The Supporting Information is available free of charge at https://pubs.acs.org/doi/10.1021/acscatal.0c04748.

Experimental procedures and compound characterization data including ^{1}H, ^{19}F, ^{13}C NMR spectra (CIF)

General remarks, synthesis of BCPs, optimizations for the iron-catalyzed C−H activation with BCPs, general procedure for the iron-catalyzed C−H activation with BCPs, characterization of product 3, characterization of products 7 and 8, characterization of product 4, removal of TAH, competition experiments, intermolecular KIE study, isotopically labelled experiments, mechanistic proposal for the formation of 3kf′, mechanistic proposal for the dimethylmethylene TAM group removal during catalysis, Mößbauer spectroscopy, X-Ray crystallographic analysis, and NMR spectra (PDF)

■ AUTHOR INFORMATION

Corresponding Author

Lutz Ackermann − *Institut für Organische und Biomolekulare Chemie and WISCh (Wöhler-Research Institute for Sustainable Chemistry), Georg-August-Universität Göttingen, 37077 Göttingen, Germany;* orcid.org/0000-0001-7034-8772; Email: Lutz.Ackermann@chemie.uni-goettingen.de

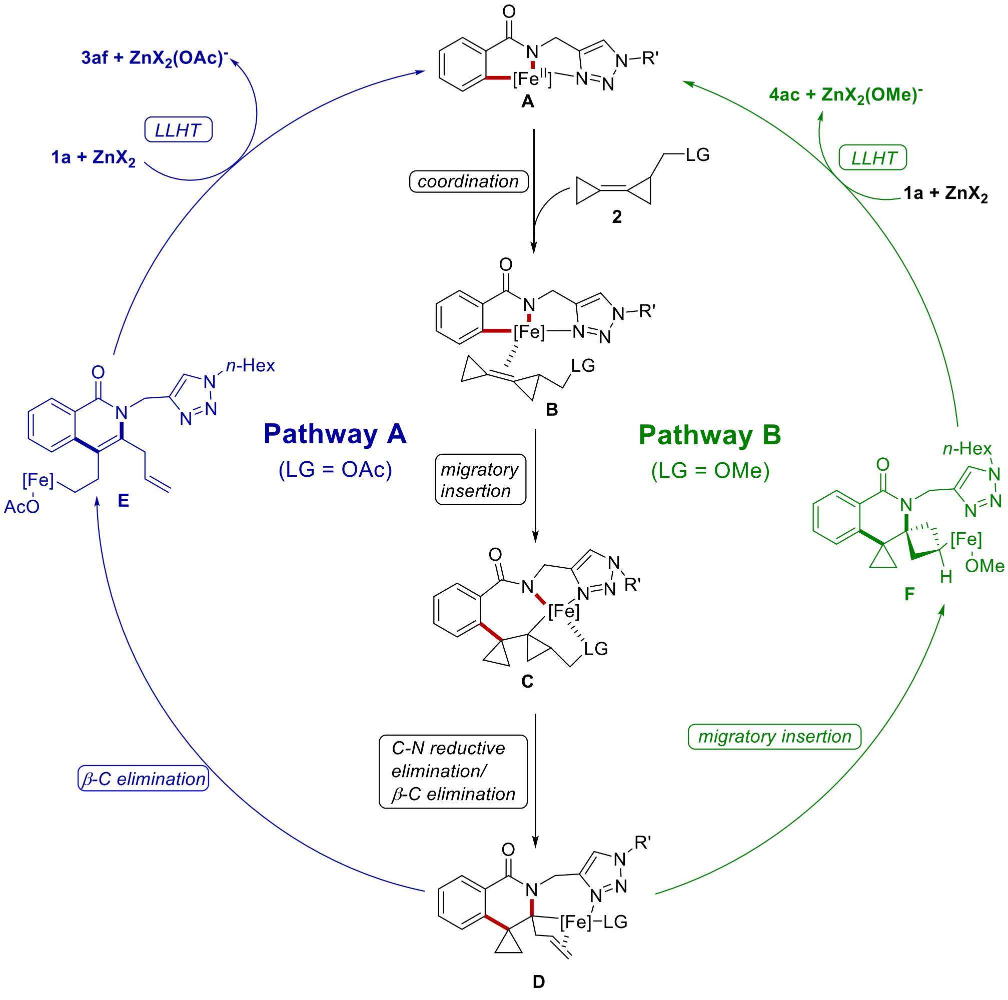

Figure 2. Proposed mechanism for iron-catalyzed C−H/C−C functionalization with BCPs **2**.

Authors

Jiayu Mo − *Institut für Organische und Biomolekulare Chemie, Georg-August-Universität Göttingen, 37077 Göttingen, Germany*

Antonis M. Messinis − *Institut für Organische und Biomolekulare Chemie, Georg-August-Universität Göttingen, 37077 Göttingen, Germany*

João C. A. Oliveira − *Institut für Organische und Biomolekulare Chemie, Georg-August-Universität Göttingen, 37077 Göttingen, Germany*

Serhiy Demeshko − *Institut für Anorganische Chemie, Georg-August-Universität Göttingen, 37077 Göttingen, Germany*

Franc Meyer − *Institut für Anorganische Chemie and WISCh (Wöhler-Research Institute for Sustainable Chemistry), Georg-August-Universität Göttingen, 37077 Göttingen, Germany;* orcid.org/0000-0002-8613-7862

Complete contact information is available at:
https://pubs.acs.org/10.1021/acscatal.0c04748

Author Contributions

J.M. and A.M.M. contributed equally to this work. The manuscript was written through contributions of all authors.

Notes

The authors declare no competing financial interest.

■ ACKNOWLEDGMENTS

Generous support by the DFG (Gottfried-Wilhelm-Leibniz award to L.A.) and the CSC (fellow-ship to J.M.) is gratefully acknowledged. We thank Dr. Christopher Golz (Göttingen University) for assistance with the X-ray diffraction analysis.

■ REFERENCES

(1) Rej, S.; Ano, Y.; Chatani, N. Bidentate Directing Groups: An Efficient Tool in C−H Bond Functionalization Chemistry for the Expedient Construction of C−C Bonds. *Chem. Rev.* **2020**, *120*, 1788−1887.

(2) Sambiagio, C.; Schönbauer, D.; Blieck, R.; Dao-Huy, T.; Pototschnig, G.; Schaaf, P.; Wiesinger, T.; Zia, M. F.; Wencel-Delord, J.; Besset, T.; Maes, B. U. W.; Schnürch, M. A Comprehensive Overview of Directing Groups Applied in Metal-Catalysed C−H Functionalisation Chemistry. *Chem. Soc. Rev.* **2018**, *47*, 6603−6743.

(3) Davies, H. M. L.; Morton, D. Collective Approach to Advancing C−H Functionalization. *ACS Cent. Sci.* **2017**, *3*, 936−943.

(4) He, J.; Wasa, M.; Chan, K. S. L.; Shao, Q.; Yu, J.-Q. Palladium-Catalyzed Transformations of Alkyl C−H Bonds. *Chem. Rev.* **2017**, *117*, 8754−8786.

(5) Hartwig, J. F.; Larsen, M. A. Undirected, Homogeneous C−H Bond Functionalization: Challenges and Opportunities. *ACS Cent. Sci.* **2016**, *2*, 281−292.

(6) Rouquet, G.; Chatani, N. Catalytic Functionalization of C(sp^2)−H and C(sp^3)−H Bonds by Using Bidentate Directing Groups. *Angew. Chem., Int. Ed.* **2013**, *52*, 11726−11743.

(7) Neufeldt, S. R.; Sanford, M. S. Controlling Site Selectivity in Palladium-Catalyzed C−H Bond Functionalization. *Acc. Chem. Res.* **2012**, *45*, 936−946.

(8) McMurray, L.; O'Hara, F.; Gaunt, M. J. Recent Developments in Natural Product Synthesis using Metal-Catalysed C−H Bond Functionalisation. *Chem. Soc. Rev.* **2011**, *40*, 1885−1898.

(9) Lyons, T. W.; Sanford, M. S. Palladium-Catalyzed Ligand-Directed C−H Functionalization Reactions. *Chem. Rev.* **2010**, *110*, 1147−1169.

(10) Daugulis, O.; Do, H.-Q.; Shabashov, D. Palladium- and Copper-Catalyzed Arylation of Carbon−Hydrogen Bonds. *Acc. Chem. Res.* **2009**, *42*, 1074−1086.

(11) Pouliot, J.-R.; Grenier, F.; Blaskovits, J. T.; Beaupré, S.; Leclerc, M. Direct (Hetero)arylation Polymerization: Simplicity for Conjugated Polymer Synthesis. *Chem. Rev.* **2016**, *116*, 14225−14274.

(12) Schipper, D. J.; Fagnou, K. Direct Arylation as a Synthetic Tool for the Synthesis of Thiophene-Based Organic Electronic Materials. *Chem. Mater.* **2011**, *23*, 1594−1600.

(13) Welin, E. R.; Ngamnithiporn, A.; Klatte, M.; Lapointe, G.; Pototschnig, G. M.; McDermott, M. S. J.; Conklin, D.; Gilmore, C. D.; Tadross, P. M.; Haley, C. K.; Negoro, K.; Glibstrup, E.; Grünanger, C. U.; Allan, K. M.; Virgil, S. C.; Slamon, D. J.; Stoltz, B. M. Concise Total Syntheses of (−)-Jorunnamycin A and (−)-Jorumycin enabled by Asymmetric Catalysis. *Science* **2019**, *363*, 270−275.

(14) Yamaguchi, J.; Yamaguchi, A. D.; Itami, K. C−H Bond Functionalization: Emerging Synthetic Tools for Natural Products and Pharmaceuticals. *Angew. Chem., Int. Ed.* **2012**, *51*, 8960−9009.

(15) Friis, S. D.; Johansson, M. J.; Ackermann, L. Cobalt-Catalysed C−H Methylation for Late-Stage Drug Diversification. *Nat. Chem.* **2020**, *12*, 511−519.

(16) Cernak, T.; Dykstra, K. D.; Tyagarajan, S.; Vachal, P.; Krska, S. W. The Medicinal Chemist's Toolbox for Late Stage Functionalization of Drug-like Molecules. *Chem. Soc. Rev.* **2016**, *45*, 546−576.

(17) Seki, M. A New Catalytic System for Ru-Catalyzed C−H Arylation Reactions and Its Application in the Practical Syntheses of Pharmaceutical Agents. *Org. Process Res. Dev.* **2016**, *20*, 867−877.

(18) Ackermann, L. Robust Ruthenium(II)-Catalyzed C−H Arylations: Carboxylate Assistance for the Efficient Synthesis of Angiotensin-II-Receptor Blockers. *Org. Process Res. Dev.* **2015**, *19*, 260−269.

(19) Gandeepan, P.; Müller, T.; Zell, D.; Cera, G.; Warratz, S.; Ackermann, L. 3d Transition Metals for C−H Activation. *Chem. Rev.* **2019**, *119*, 2192−2452.

(20) Nakao, Y. Hydroarylation of C−C Multiple Bonds Using Nickel Catalysts. In *Catalytic Hydroarylation of Carbon−Carbon Multiple Bonds*; Ackermann, L., Gunnoe, T. B., Habgood, L. G., Eds.; Wiley-VCH: Weinheim, 2018; pp 175−192.

(21) Hu, Y.; Zhou, B.; Wang, C. Inert C−H Bond Transformations Enabled by Organometallic Manganese Catalysis. *Acc. Chem. Res.* **2018**, *51*, 816−827.

(22) Kommagalla, Y.; Chatani, N. Cobalt(II)-Catalyzed C−H Functionalization using an N,N′-Bidentate Directing Group. *Coord. Chem. Rev.* **2017**, *350*, 117−135.

(23) Moselage, M.; Li, J.; Ackermann, L. Cobalt-Catalyzed C−H Activation. *ACS Catal.* **2016**, *6*, 498−525.

(24) Yamaguchi, J.; Muto, K.; Itami, K. Nickel-Catalyzed Aromatic C−H Functionalization. *Top. Curr. Chem.* **2016**, *374*, 157−189.

(25) Castro, L. C. M.; Chatani, N. Nickel Catalysts/N,N′-Bidentate Directing Groups: An Excellent Partnership in Directed C−H Activation Reactions. *Chem. Lett.* **2015**, *44*, 410−421.

(26) Jackson, E. P.; Malik, H. A.; Sormunen, G. J.; Baxter, R. D.; Liu, P.; Wang, H.; Shareef, A.-R.; Montgomery, J. Mechanistic Basis for Regioselection and Regiodivergence in Nickel-Catalyzed Reductive Couplings. *Acc. Chem. Res.* **2015**, *48*, 1736−1745.

(27) Gao, K.; Yoshikai, N. Low-Valent Cobalt Catalysis: New Opportunities for C−H Functionalization. *Acc. Chem. Res.* **2014**, *47*, 1208−1219.

(28) Kulkarni, A. A.; Daugulis, O. Direct Conversion of Carbon-Hydrogen into Carbon-Carbon Bonds by First-Row Transition-Metal Catalysis. *Synthesis* **2009**, 4087−4109.

(29) Piontek, A.; Bisz, E.; Szostak, M. Iron-Catalyzed Cross-Couplings in the Synthesis of Pharmaceuticals: In Pursuit of Sustainability. *Angew. Chem., Int. Ed.* **2018**, *57*, 11116−11128.

(30) Bisz, E.; Szostak, M. Iron-Catalyzed C−O Bond Activation: Opportunity for Sustainable Catalysis. *ChemSusChem* **2017**, *10*, 3964−3981.

(31) Shang, R.; Ilies, L.; Nakamura, E. Iron-Catalyzed C−H Bond Activation. *Chem. Rev.* **2017**, *117*, 9086−9139.

(32) Yoshikai, N. Iron-Catalyzed C−C Bond Formation via Chelation-Assisted C−H Activation. *Isr. J. Chem.* **2017**, *57*, 1117−1130.

(33) Fürstner, A. Iron Catalysis in Organic Synthesis: A Critical Assessment of What It Takes To Make This Base Metal a Multitasking Champion. *ACS Cent. Sci.* **2016**, *2*, 778−789.

(34) Cera, G.; Ackermann, L. Iron-Catalyzed C−H Functionalization Processes. *Top. Curr. Chem.* **2016**, *374*, 57.

(35) Bauer, I.; Knölker, H.-J. Iron Catalysis in Organic Synthesis. *Chem. Rev.* **2015**, *115*, 3170−3387.

(36) Sun, C.-L.; Li, B.-J.; Shi, Z.-J. Direct C−H Transformation via Iron Catalysis. *Chem. Rev.* **2011**, *111*, 1293−1314.

(37) Correa, A.; García Mancheño, O.; Bolm, C. Iron-Catalysed Carbon−Heteroatom and Heteroatom−Heteroatom Bond Forming Processes. *Chem. Soc. Rev.* **2008**, *37*, 1108−1117 and references therein.

(38) Messinis, A. M.; Finger, L. H.; Hu, L.; Ackermann, L. Allenes for Versatile Iron-Catalyzed C−H Activation by Weak O-Coordination: Mechanistic Insights by Kinetics, IntermediateIsolation, and Computation. *J. Am. Chem. Soc.* **2020**, *142*, 13102−13111.

(39) Mo, J.; Müller, T.; Oliveira, J. C. A.; Demeshko, S.; Meyer, F.; Ackermann, L. Iron-Catalyzed C−H Activation with Propargyl Acetates: Mechanistic Insights into Iron(II) by Experiment, Kinetics, Mössbauer Spectroscopy, and Computation. *Angew. Chem., Int. Ed.* **2019**, *58*, 12874−12878.

(40) Mo, J.; Müller, T.; Oliveira, J. C. A.; Ackermann, L. 1, 4-Iron Migration for Expedient Allene Annulations through Iron-Catalyzed C−H/N−H/C−O/C−H Functionalizations. *Angew. Chem., Int. Ed.* **2018**, *57*, 7719−7723.

(41) Guo, S.; AbuSalim, D. I.; Cook, S. P. Aqueous Benzylic C−H Trifluoromethylation for Late-Stage Functionalization. *J. Am. Chem. Soc.* **2018**, *140*, 12378−12382.

(42) Kimura, N.; Kochi, T.; Kakiuchi, F. Iron-Catalyzed Regioselective Anti-Markovnikov Addition of C−H Bonds in Aromatic Ketones to Alkenes. *J. Am. Chem. Soc.* **2017**, *139*, 14849−14852.

(43) Yu, R. P.; Hesk, D.; Rivera, N.; Pelczer, I.; Chirik, P. J. Iron-Catalysed Tritiation of Pharmaceuticals. *Nature* **2016**, *529*, 195.

(44) Osberger, T. J.; Rogness, D. C.; Kohrt, J. T.; Stepan, A. F.; White, M. C. Oxidative Diversification of Amino Acids and Peptides by Small-Molecule Iron Catalysis. *Nature* **2016**, *537*, 214−219.

(45) Bornschein, C.; Werkmeister, S.; Wendt, B.; Jiao, H.; Alberico, E.; Baumann, W.; Junge, H.; Junge, K.; Beller, M. Mild and Selective Hydrogenation of Aromatic and Aliphatic (di)Nitriles with a Well-defined Iron Pincer Complex. *Nat. Commun.* **2014**, *5*, 4111.

(46) Jagadeesh, R. V.; Surkus, A.-E.; Junge, H.; Pohl, M.-M.; Radnik, J.; Rabeah, J.; Huan, H.; Schunemann, V.; Brückner, A.; Beller, M. Nanoscale Fe_2O_3-Based Catalysts for Selective Hydrogenation of Nitroarenes to Anilines. *Science* **2013**, *342*, 1073−1076.

(47) Egorova, K. S.; Ananikov, V. P. Which Metals are Green for Catalysis? Comparison of the Toxicities of Ni, Cu, Fe, Pd, Pt, Rh, and Au Salts. *Angew. Chem., Int. Ed.* **2016**, *55*, 12150−12162.

(48) Groendyke, B. J.; AbuSalim, D. I.; Cook, S. P. Iron-Catalyzed, Fluoroamide-Directed C−H Fluorination. *J. Am. Chem. Soc.* **2016**, *138*, 12771−12774.

(49) Jia, T.; Zhao, C.; He, R.; Chen, H.; Wang, C. Iron-Carbonyl-Catalyzed Redox-Neutral [4+2] Annulation of N−H Imines and Internal Alkynes by C−H Bond Activation. *Angew. Chem., Int. Ed.* **2016**, *55*, 5268−5271.

(50) Shang, R.; Ilies, L.; Nakamura, E. Iron-Catalyzed Ortho C−H Methylation of Aromatics Bearing a Simple Carbonyl Group with Methylaluminum and Tridentate Phosphine Ligand. *J. Am. Chem. Soc.* **2016**, *138*, 10132−10135.

(51) Ilies, L.; Matsubara, T.; Ichikawa, S.; Asako, S.; Nakamura, E. Iron-Catalyzed Directed Alkylation of Aromatic and Olefinic Carboxamides with Primary and Secondary Alkyl Tosylates, Mesylates, and Halides. *J. Am. Chem. Soc.* **2014**, *136*, 13126−13129.

(52) Monks, B. M.; Fruchey, E. R.; Cook, S. P. Iron-catalyzed C(sp^2)−H Alkylation of Carboxamides with Primary Electrophiles. *Angew. Chem., Int. Ed.* **2014**, *53*, 11065−11069.

(53) Matsubara, T.; Asako, S.; Ilies, L.; Nakamura, E. Synthesis of Anthranilic Acid Derivatives through Iron-Catalyzed Ortho Amination of Aromatic Carboxamides with N-Chloroamines. *J. Am. Chem. Soc.* **2014**, *136*, 646−649.

(54) Fruchey, E. R.; Monks, B. M.; Cook, S. P. A Unified Strategy for Iron-Catalyzed ortho-Alkylation of Carboxamides. *J. Am. Chem. Soc.* **2014**, *136*, 13130−13133 and references therein.

(55) Cohen, Y.; Cohen, A.; Marek, I. Creating Stereocenters within Acyclic Systems by C−C Bond Cleavage of Cyclopropanes. *Chem. Rev.* **2020**, DOI: 10.1021/acs.chemrev.0c00167.

(56) Nairoukh, Z.; Cormier, M.; Marek, I. Merging C−H and C−C bond Cleavage in Organic Synthesis. *Nat. Rev. Chem.* **2017**, *1*, 0035.

(57) Souillart, L.; Cramer, N. Catalytic C−C Bond Activations via Oxidative Addition to Transition Metals. *Chem. Rev.* **2015**, *115*, 9410−9464.

(58) Xu, T.; Dermenci, A.; Dong, G. Transition Metal-Catalyzed C−C Bond Activation of Four-Membered Cyclic Ketones. *Top. Curr. Chem.* **2014**, *346*, 233−257.

(59) Seiser, T.; Saget, T.; Tran, D. N.; Cramer, N. Cyclobutanes in Catalysis. *Angew. Chem., Int. Ed.* **2011**, *50*, 7740−7752.

(60) Murakami, M.; Matsuda, T. Metal-Catalysed Cleavage of Carbon−Carbon Bonds. *Chem. Commun.* **2011**, *47*, 1100−1105.

(61) Deng, L.; Chen, M.; Dong, G. Concise Synthesis of (−)-Cycloclavine and (−)-5-epi-Cycloclavine via Asymmetric C−C Activation. *J. Am. Chem. Soc.* **2018**, *140*, 9652−9658.

(62) Xia, Y.; Lu, G.; Liu, P.; Dong, G. Catalytic Activation of Carbon−Carbon Bonds in Cyclopentanones. *Nature* **2016**, *539*, 546−550.

(63) Deng, L.; Xu, T.; Li, H.; Dong, G. Enantioselective Rh-Catalyzed Carboacylation of C=N Bonds via C−C Activation of Benzocyclobutenones. *J. Am. Chem. Soc.* **2016**, *138*, 369−374.

(64) Matsuda, T.; Kato, K.; Goya, T.; Shimada, S.; Murakami, M. Ruthenium-Catalyzed Cycloisomerization of 2, 2′-Diethynyl-biphenyls Involving Cleavage of a Carbon-Carbon Triple Bond. *Chem.—Eur. J.* **2016**, *22*, 1941−1943.

(65) Zhou, X.; Dong, G. (4+1) vs (4+2): Catalytic Intramolecular Coupling between Cyclobutanones and Trisubstituted Allenes via C−C Activation. *J. Am. Chem. Soc.* **2015**, *137*, 13715−13721.

(66) Zeng, R.; Dong, G. Rh-Catalyzed Decarbonylative Coupling with Alkynes via C−C Activation of Isatins. *J. Am. Chem. Soc.* **2015**, *137*, 1408−1411.

(67) Ding, L.; Ishida, N.; Murakami, M.; Morokuma, K. sp^3−sp^2 vs sp^3−sp^3 C−C Site Selectivity in Rh-Catalyzed Ring Opening of Benzocyclobutenol: A DFT Study. *J. Am. Chem. Soc.* **2014**, *136*, 169−178.

(68) Ishida, N.; Ikemoto, W.; Murakami, M. Cleavage of C−C and C−Si σ-Bonds and Their Intramolecular Exchange. *J. Am. Chem. Soc.* **2014**, *136*, 5912−5915.

(69) Ko, H. M.; Dong, G. Cooperative Activation of Cyclobutanones and Olefins Leads to Bridged-Ring Systems by a Catalytic [4+2] Coupling. *Nat. Chem.* **2014**, *6*, 739−744.

(70) Yada, A.; Fujita, S.; Murakami, M. Enantioselective Insertion of a Carbenoid Carbon into a C−C Bond to Expand Cyclobutanols to Cyclopentanols. *J. Am. Chem. Soc.* **2014**, *136*, 7217−7220.

(71) Souillart, L.; Cramer, N. Highly Enantioselective Rhodium(I)-Catalyzed Carbonyl Carboacylations Initiated by C−C Bond Activation. *Angew. Chem., Int. Ed.* **2014**, *53*, 9640−9644.

(72) Souillart, L.; Parker, E.; Cramer, N. Highly Enantioselective Rhodium(I)-Catalyzed Carbonyl Carboacylations Initiated by C−C Bond Activation. *Angew. Chem., Int. Ed.* **2014**, *53*, 3001−3005.

(73) Souillart, L.; Cramer, N. Exploitation of Rh(I)−Rh(III) Cycles in Enantioselective C−C bond Cleavages: Access to β-tetralones and Benzobicyclo[2.2.2]octanones. *Chem. Sci.* **2014**, *5*, 837−840.

(74) Masuda, Y.; Hasegawa, M.; Yamashita, M.; Nozaki, K.; Ishida, N.; Murakami, M. Oxidative Addition of a Strained C−C Bond onto

Electron-Rich Rhodium(I) at Room Temperature. *J. Am. Chem. Soc.* **2013**, *135*, 7142−7145.

(75) Ishida, N.; Sawano, S.; Masuda, Y.; Murakami, M. Rhodium-Catalyzed Ring Opening of Benzocyclobutenols with Site-Selectivity Complementary to Thermal Ring Opening. *J. Am. Chem. Soc.* **2012**, *134*, 17502−17504.

(76) Liu, L.; Ishida, N.; Murakami, M. Atom- and Step-economical Pathway to Chiral Benzobicyclo[2.2.2]octenones through Carbon-Carbon Bond Cleavage. *Angew. Chem., Int. Ed.* **2012**, *51*, 2485−2488.

(77) Seiser, T.; Cramer, N. Rhodium-Catalyzed C−C Bond Cleavage: Construction of Acyclic Methyl Substituted Quaternary Stereogenic Centers. *J. Am. Chem. Soc.* **2010**, *132*, 5340−5341.

(78) Wender, P. A.; Takahashi, H.; Witulski, B. Transition Metal Catalyzed [5 + 2] Cycloadditions of Vinylcyclopropanes and Alkynes: A Homolog of the Diels-Alder Reaction for the Synthesis of Seven-Membered Rings. *J. Am. Chem. Soc.* **1995**, *117*, 4720−4721.

(79) Murakami, M.; Amii, H.; Ito, Y. Selective Activation of Carbon−Carbon Bonds Next to a Carbonyl Group. *Nature* **1994**, *370*, 540−541.

(80) Li, Q.; Yuan, X.; Li, B.; Wang, B. The Regioselective Annulation of Alkylidenecyclopropanes by Rh(III)-Catalyzed C−H/C−C Activation to Access Spirocyclic Benzosultams. *Chem. Commun.* **2020**, *56*, 1835−1838.

(81) Wang, Q.; Shi, L.; Liu, S.; Zhi, C.; Fu, L.-R.; Zhu, X.; Hao, X.-Q.; Song, M.-P. Solvent-free and Room Temperature Microwave-assisted Direct C7 Allylation of Indolines via Sequential C−H and C−C Activation. *RSC Adv.* **2020**, *10*, 10883−10887.

(82) Wang, Q.; Zhi, C. L.; Lu, P. P.; Liu, S.; Zhu, X.; Hao, X. Q.; Song, M. P. Rhodium(III)-Catalyzed Direct C7 Allylation of Indolines via Sequential C−H and C−C Activation. *Adv. Synth. Catal.* **2019**, *361*, 1253−1258.

(83) Hu, Z.; Hu, X.-Q.; Zhang, G.; Gooßen, L. J. Ring-Opening Ortho-C−H Allylation of Benzoic Acids with Vinylcyclopropanes: Merging Catalytic C−H and C−C Activation Concepts. *Org. Lett.* **2019**, *21*, 6770−6773.

(84) Zhu, Y. Q.; Niu, Y. X.; Hui, L. W.; He, J. L.; Zhu, K. Reaction of Isoquinolin-1(2H)-Ones with Methylenecyclopropanes via Rhodium-(III)-Catalyzed C−H Activation. *Adv. Synth. Catal.* **2019**, *361*, 2897−2903.

(85) Wu, J.-Q.; Qiu, Z.-P.; Zhang, S.-S.; Liu, J.-G.; Lao, Y.-X.; Gu, L.-Q.; Huang, Z.-S.; Li, J.; Wang, H. Rhodium(III)-Catalyzed C−H/C−C Activation Sequence: Vinylcyclopropanes as Versatile Synthons in Direct C−H Allylation Reactions. *Chem. Commun.* **2015**, *51*, 77−80.

(86) Masarwa, A.; Weber, M.; Sarpong, R. Selective C−C and C−H Bond Activation/Cleavage of Pinene Derivatives: Synthesis of Enantiopure Cyclohexenone Scaffolds and Mechanistic Insights. *J. Am. Chem. Soc.* **2015**, *137*, 6327−6334.

(87) Cui, S.; Zhang, Y.; Wu, Q. Rh(III)-Catalyzed C−H Activation/Cycloaddition of Benzamides and Methylenecyclopropanes: Divergence in Ring Formation. *Chem. Sci.* **2013**, *4*, 3421−3426.

(88) Seiser, T.; Roth, O. A.; Cramer, N. Enantioselective Synthesis of Indanols from tert-Cyclobutanols Using a Rhodium-Catalyzed C−C/C−H Activation Sequence. *Angew. Chem., Int. Ed.* **2009**, *48*, 6320−6323.

(89) Aïssa, C.; Fürstner, A. A Rhodium-Catalyzed C−H Activation/Cycloisomerization Tandem. *J. Am. Chem. Soc.* **2007**, *129*, 14836−14837.

(90) Liang, Y.-F.; Müller, V.; Liu, W.; Münch, A.; Stalke, D.; Ackermann, L. Methylenecyclopropane Annulation by Manganese(I)-Catalyzed Stereoselective C−H/C−C Activation. *Angew. Chem., Int. Ed.* **2017**, *56*, 9415−9419.

(91) Lu, Q.; Klauck, F. J. R.; Glorius, F. Manganese-Catalyzed Allylation via Sequential C−H and C−C/C−Het bond Activation. *Chem. Sci.* **2017**, *8*, 3379−3383.

(92) Meyer, T. H.; Liu, W.; Feldt, M.; Wuttke, A.; Mata, R. A.; Ackermann, L. Manganese(I)-Catalyzed Dispersion-Enabled C−H/C−C Activation. *Chem.—Eur. J.* **2017**, *23*, 5443−5447.

(93) Zell, D.; Bu, Q.; Feldt, M.; Ackermann, L. Mild C−H/C−C Activation by Z-Selective Cobalt Catalysis. *Angew. Chem., Int. Ed.* **2016**, *55*, 7408−7412.

(94) Li, M.; Kwong, F. Y. Cobalt-Catalyzed Tandem C−H Activation/C−C Cleavage/C−H Cyclization of Aromatic Amides with Alkylidenecyclopropanes. *Angew. Chem., Int. Ed.* **2018**, *57*, 6512−6516.

(95) Brandi, A.; Cicchi, S.; Cordero, F. M.; Goti, A. Progress in the Synthesis and Transformations of Alkylidenecyclopropanes and Alkylidenecyclobutanes. *Chem. Rev.* **2014**, *114*, 7317−7420.

(96) Pellissier, H. Recent Developments in the Reactivity of Methylene- and Alkylidenecyclopropane Derivatives. *Tetrahedron* **2010**, *66*, 8341−8375.

(97) Goti, A.; Cordero, F. M.; Brandi, A. Cycloadditions onto Methylene- and Alkylidenecyclopropane Derivatives. *Top. Curr. Chem.* **2005**, *178*, 1−97.

(98) Brandi, A.; Cicchi, S.; Cordero, F. M.; Goti, A. Heterocycles from Alkylidenecyclopropanes. *Chem. Rev.* **2003**, *103*, 1213−1270.

(99) de Meijere, A.; Kozhushkov, S. I. An Evolving Multifunctional Molecular Building Block: Bicyclopropylidene. *Eur. J. Org. Chem.* **2000**, *2000*, 3809−3822.

(100) de Meijere, A.; Kozhushkov, S. I.; Khlebnikov, A. F. Bicyclopropylidene−A Unique Tetrasubstituted Alkene and a Versatile C_6-Building Block. *Top. Curr. Chem.* **2000**, *207*, 89−147.

(101) de Meijere, A.; Kozhushkov, S. I.; Khlebnikov, A. F. The Chemistry of Bicyclopropylidene. *Russ. J. Org. Chem.* **1996**, *32*, 1555−1575.

(102) de Meijere, A.; Kozhushkov, S. I.; Späth, T. Bicyclopropylidene: Cyclopropane, cyclopropylidene. *Org. Synth.* **2003**, *78*, 142.

(103) Schinkel, M.; Wallbaum, J.; Kozhushkov, S. I.; Marek, I.; Ackermann, L. Carboxylate Assistance for Catalyzed Hydroarylations of Methylenecyclopropanes. *Org. Lett.* **2013**, *15*, 4482−4484.

(104) Ackermann, L.; Kozhushkov, S. I.; Yufit, D. S. Ruthenium-Catalyzed Hydroarylation of Methylenecyclopropanes through C−H Bond Cleavage: Scope and Mechanism. *Eur. J. Org. Chem.* **2012**, *18*, 12068−12077.

(105) Kozhushkov, S. I.; Yufit, D. S.; Ackermann, L. Ruthenium-Catalyzed Hydroarylations of Methylenecyclopropanes: Mild C−H Bond Functionalizations with Conservation of Cyclopropane Rings. *Org. Lett.* **2008**, *10*, 3409−3412.

(106) Korvorapun, K.; Moselage, M.; Struwe, J.; Rogge, T.; Messinis, A. M.; Ackermann, L. Regiodivergent C−H and Decarboxylative Alkylation by Ruthenium Catalysis: Ortho Versus Meta Position-Selectivity. *Angew. Chem., Int. Ed.* **2020**, *59*, 18795−18803.

(107) Moselage, M.; Li, J.; Kramm, F.; Ackermann, L. Ruthenium-(II)-Catalyzed C−C Arylations and Alkylations: Decarbamoylative C−C Functionalizations. *Angew. Chem., Int. Ed.* **2017**, *56*, 5341−5344.

(108) Under otherwise identical conditions, the use of the parent unsubstituted BCP, gave thus far less satisfactory results.

(109) Gandeepan, P.; Kaplaneris, N.; Santoro, S.; Vaccaro, L.; Ackermann, L. Biomass-Derived Solvents for Sustainable Transition Metal-Catalyzed C−H Activation. *ACS Sustainable Chem. Eng.* **2019**, *7*, 8023−8040.

(110) Li, G.; Ma, S.; Szostak, M. Amide Bond Activation: The Power of Resonance. *Trends Chem.* **2020**, *2*, 914−928.

(111) Gütlich, P.; Bill, E.; Trautwein, A. X. *Mössbauer Spectroscopy and Transition Metal Chemistry: Fundamentals and Applications*; Springer-Verlag: Berlin, 2011.

(112) Muñoz, S. B., III; Daifuku, S. L.; Brennessel, W. W.; Neidig, M. L. Isolation, Characterization, and Reactivity of $Fe_8Me_{12}^-$: Kochi's S = 1/2 Species in Iron-Catalyzed Cross-Couplings with MeMgBr and Ferric Salts. *J. Am. Chem. Soc.* **2016**, *138*, 7492−7495.

(113) Boddie, T. E.; Carpenter, S. H.; Baker, T. M.; DeMuth, J. C.; Cera, G.; Brennessel, W. W.; Ackermann, L.; Neidig, M. L. Identification and Reactivity of Cyclometalated Iron(II) Intermediates in Triazole-Directed Iron-Catalyzed C−H Activation. *J. Am. Chem. Soc.* **2019**, *141*, 12338−12345.

(114) Tao, J.; Perdew, J. P.; Staroverov, V. N.; Scuseria, G. E. Climbing the Density Functional Ladder: Nonempirical Meta-Generalized Gradient Approximation Designed for Molecules and Solids. *Phys. Rev. Lett.* **2003**, *91*, 146401.

(115) Grimme, S.; Ehrlich, S.; Goerigk, L. Effect of the Damping Function in Dispersion Corrected Density Functional Theory. *J. Comput. Chem.* **2011**, *32*, 1456−1465.

(116) Grimme, S.; Antony, J.; Ehrlich, S.; Krieg, H. A Consistent and Accurate ab initio Parametrization of Density Functional Dispersion Correction (DFT-D) for the 94 Elements H-Pu. *J. Chem. Phys.* **2010**, *132*, 154104.

(117) Weigend, F. Accurate Coulomb-fitting Basis Sets for H to Rn. *Phys. Chem. Chem. Phys.* **2006**, *8*, 1057−1065.

(118) Weigend, F.; Ahlrichs, R. Balanced Basis Sets of Split Valence, Triple Zeta Valence and Quadruple Zeta Valence Quality for H to Rn: Design and Assessment of Accuracy. *Phys. Chem. Chem. Phys.* **2005**, *7*, 3297−3305.

(119) Zhao, Y.; Truhlar, D. G. Design of Density Functionals That Are Broadly Accurate for Thermochemistry, Thermochemical Kinetics, and Nonbonded Interactions. *J. Phys. Chem. A* **2005**, *109*, 5656−5667.

(120) Caldeweyher, E.; Ehlert, S.; Hansen, A.; Neugebauer, H.; Spicher, S.; Bannwarth, C.; Grimme, S. A Generally Applicable Atomic-Charge Dependent London Dispersion Correction. *J. Chem. Phys.* **2019**, *150*, 154122.

(121) Caldeweyher, E.; Bannwarth, C.; Grimme, S. Extension of the D3 Dispersion Coefficient Model. *J. Chem. Phys.* **2017**, *147*, 034112.

(122) https://www.chemie.uni-bonn.de/pctc/mulliken-center/software/dftd4 (accessed November 10, 2020).

(123) Marenich, A. V.; Cramer, C. J.; Truhlar, D. G. Universal Solvation Model Based on Solute Electron Density and on a Continuum Model of the Solvent Defined by the Bulk Dielectric Constant and Atomic Surface Tensions. *J. Phys. Chem. B* **2009**, *113*, 6378−6396.

(124) Tang, S.; Eisenstein, O.; Nakao, Y.; Sakaki, S. Aromatic C−H σ-Bond Activation by Ni^0, Pd^0, and Pt^0 Alkene Complexes: Concerted Oxidative Addition to Metal vs Ligand-to-Ligand H Transfer Mechanism. *Organometallics* **2017**, *36*, 2761−2771.

(125) Eisenstein, O.; Milani, J.; Perutz, R. N. Selectivity of C−H Activation and Competition between C−H and C−F Bond Activation at Fluorocarbons. *Chem. Rev.* **2017**, *117*, 8710−8753.

(126) Zhu, C.; Stangier, M.; Oliveira, J. C. A.; Massignan, L.; Ackermann, L. Iron-Electrocatalyzed C−H Arylations: Mechanistic Insights into Oxidation-Induced Reductive Elimination for Ferraelectrocatalysis. *Chem.—Eur. J.* **2019**, *25*, 16382−16389.

(127) Zell, D.; Bursch, M.; Müller, V.; Grimme, S.; Ackermann, L. Full Selectivity Control in Cobalt(III)-Catalyzed C−H Alkylations by Switching of the C−H Activation Mechanism. *Angew. Chem., Int. Ed.* **2017**, *56*, 10378−10382.

(128) Loup, J.; Zell, D.; Oliveira, J. C. A.; Keil, H.; Stalke, D.; Ackermann, L. Asymmetric Iron-Catalyzed C−H Alkylation Enabled by Remote Ligand Meta-Substitution. *Angew. Chem., Int. Ed.* **2017**, *56*, 14197−14201.